Using ϕ-meson elliptic flow to map the strength of the partonic interaction

Md. Nasim
National Institute of Science Education and Research, Bhubaneswar 751005, India
(Received 11 December 2013; revised manuscript received 16 February 2014; published 19 March 2014)

A compilation of recently measured STAR data for elliptic flow (v_2) of ϕ mesons in the Relativistic Heavy Ion Collider (RHIC) Beam Energy Scan program and comparison with a multiphase transport model (AMPT) are presented. The experimental data at $\sqrt{s_{NN}} \geqslant 19.6$ GeV agree well with the string melting version of the AMPT model. The model includes partonic interactions and quark coalescence as a mechanism of hadronization. This indicates that there is a substantial contribution to collectivity from partonic interactions at $\sqrt{s_{NN}} \geqslant 19.6$ GeV. The measured ϕ-meson v_2 at $\sqrt{s_{NN}} = 7.7$ and 11.5 GeV are found to be smaller than those obtained from the AMPT model without partonic interactions. This indicates negligible contribution of partonic collectivity to the observed ϕ-meson v_2 at $\sqrt{s_{NN}} \leqslant 11.5$ GeV.

DOI: 10.1103/PhysRevC.89.034909 PACS number(s): 25.75.Ld

I. INTRODUCTION

One of the main goals of high energy heavy-ion collision experiments is to study the various aspects of the QCD phase diagram [1]. With this purpose the Relativistic Heavy Ion Collider (RHIC) has finished the first phase of the Beam Energy Scan (BES) program [2–4]. The aim of the BES program was to look for changes in observation of various measurements as a function of beam energy to establish the transition region between the partonic and/or hadronic dominant interactions in the QCD phase diagram [5].

The elliptic flow parameter v_2 is a good tool for studying the system formed in the early stages of high energy collisions at RHIC [6–10]. It describes the azimuthal momentum anisotropy of particle emission in heavy-ion collisions. It is defined as the second harmonic coefficient of the azimuthal Fourier decomposition of the momentum distribution with respect to the reaction plane angle (Ψ), and can be written as

$$v_2 = \langle \cos[2(\phi - \Psi)] \rangle, \tag{1}$$

where ϕ is emission azimuthal angle [11]. According to hydrodynamical description, v_2 is an early time phenomenon and sensitive to the equation of state of the system formed in the collision [6–10,12]. The results from the RHIC on v_2 as a function of transverse momentum (p_T) show that at low p_T elliptic flow of identified hadrons follows mass ordering (lower v_2 for heavier hadrons than for lighter hadrons) whereas at intermediate p_T all mesons and all baryons form two different groups. When v_2 and p_T are scaled by the number of constituent quarks of the hadrons, the measured v_2 values are consistent with each other, as the parton coalescence or recombination models predicted [13–15]. This observation, is known as number of constituent quark scaling (NCQ scaling). This effect has been interpreted as collectivity being developed at the partonic stage of the evolution of the system in a heavy-ion collision [16].

Although the parton coalescence or recombination model can successfully explain the observed quark scaling in experimental data, one cannot say that only NCQ scaling of identified hadrons [16] is a sufficient signature for the formation of deconfined matter. The study of NCQ scaling of identified hadrons from the ultrarelativistic quantum molecular dynamics (UrQMD) model shows that the pure hadronic medium can also reproduce such scaling in v_2 [17–19]. This is due to modification of initially developed v_2 by later stage hadronic interactions [18]. So the v_2 of those particles which do not interact with hadronic interaction will be the clean and good probe for early dynamics in heavy-ion collisions. The ϕ meson, which is the bound state of s and $\bar{s}$ quarks, has a small interaction cross section with other hadrons [20] and freezes out early [1]. Due to the small hadronic interaction cross section, ϕ-meson v_2 are almost unaffected by later stage interaction, and will have negligible value if ϕ mesons are not produced via s and $\bar{s}$ quark coalescence [21,22]. Therefore, it is very important to study the ϕ-meson v_2 in the BES program at RHIC.

The paper is organized in the following way. In Sec. II, the AMPT model has been briefly discussed. Section III describes the comparison of experimentally measured ϕ-meson v_2 with the corresponding results from the AMPT model (version 1.11). Finally the summary and conclusion are given in Sec. IV.

II. THE AMPT MODEL

The AMPT model, which is a hybrid transport model, has four main stages: the initial conditions, partonic interactions, the conversion from partonic to hadronic matter, and hadronic interactions [23]. It uses the same initial conditions as HIJING [24]. Scattering among partons are modeled by Zhang's parton cascade [25], which calculates two-body parton scatterings using cross sections from pQCD with screening masses. In the default AMPT model, partons are recombined with their parent strings, and when they stop interacting the resulting strings fragment into hadrons according to the Lund string fragmentation model [26]. However, in the string melting scenario (labeled as AMPT-SM), these strings are converted to soft partons and a quark coalescence model is used to combine parton into hadrons. The evolution dynamics of the hadronic matter is described by a relativistic transport (ART) model. The interactions between the minijet partons in the AMPT default model and those between partons in the AMPT-SM

could give rise to substantial v_2. Therefore, agreement between the data and the results from AMPT-SM would indicate the contribution of partonic interactions to the measured v_2. The parton-parton interaction cross section in the string melting version of the AMPT is taken to be 3 mb and 10 mb. In this study, approximately 1.5 million events for each configuration were generated for minimum-bias Au+Au collisions.

III. RESULTS AND DISCUSSION

In this section, the ϕ-meson v_2 measured by STAR experiment at mid-rapidity ($|y| < 1.0$) for $\sqrt{s_{NN}} = 7.7$ - 200 GeV [3,4] has been compared with AMPT model. ϕ mesons are identified from the K^+ and K^- decay channel, the same method as used in experimental analysis.

A. Differential v_2

Figure 1 shows the comparison of elliptic flow of ϕ mesons in 0–80 % minimum-bias Au+Au collisions at mid-rapidity ($|y| < 1.0$) for $\sqrt{s_{NN}} = 7.7$, 11.5, 19.6, 27, 39, and 62.4 GeV with the corresponding results from the AMPT model [3,4]. The measured data points are compared with both AMPT string melting (3 mb and 10 mb parton-parton cross sections) and the AMPT default version. At $\sqrt{s_{NN}} = 62.4$ GeV experimental data are in a good agreement with the AMPT string melting model with 10 mb parton-parton cross-section. This is also true for $\sqrt{s_{NN}} = 200$ GeV as reported in Ref. [21]. The measured ϕ v_2, for $p_T < 1.5$ GeV/c, lie between 3 mb and 10 mb for the energy range $19.6 \leqslant \sqrt{s_{NN}} \leqslant 39$ GeV, but in order to explain the measurements for $p_T > 1.5$ GeV/c, a parton-parton cross section of the order of 10 mb is required. None of the above models can explain the trend of ϕ-meson v_2 at $\sqrt{s_{NN}} = 7.7$ and 11.5 GeV where the event statistics for data is also small. Since we expect that the ϕ-meson v_2 mostly reflect the collectivity from the partonic phase, therefore from the comparison of experimental data with the AMPT model one can conclude that the partonic collectivity has developed for $\sqrt{s_{NN}} \geqslant 19.6$ GeV at RHIC. However, the contribution from the partonic collectivity to the final collectivity seems negligible at $\sqrt{s_{NN}} \leqslant 11.5$ GeV.

B. p_T integrated elliptic flow ($\langle v_2 \rangle$)

The p_T integrated elliptic flow $\langle v_2 \rangle$, which is also an interesting observable, can be defined as

$$\langle v_2 \rangle = \frac{\int v_2(p_T) dN/dp_T dp_T}{\int dN/dp_T dp_T}, \tag{2}$$

i.e., the $\langle v_2 \rangle$ folds the measured v_2 versus p_T with the p_T distribution (dN/dp_T) of that particle. The p_T-averaged v_2 may have a better statistical precision than the p_T differential measurements. To calculate the $\langle v_2 \rangle$ of ϕ mesons, each $v_2(p_T)$ distribution was fitted with function (shown in Fig. 2): a third-order polynomial function and a function of the form

$$f_{v_2}(n) = \frac{an}{1 + \exp[-(p_T/n - b)/c]} - dn, \tag{3}$$

where a, b, c, and d are free parameters and n is the number of constituent quarks. This function was inspired by parametrizations of quark number scaling [27]. The p_T distribution of ϕ mesons has been fitted with a Levy function as shown in panel (b) of Fig. 2. The functional form of the Levy function is given by

$$f_{\text{Levy}}(p_T) = \frac{dN}{dy} \times \frac{(n-1)(n-2)}{2\pi nT[nT + m_0(n-2)]} \times \left(1 + \frac{\sqrt{p_T^2 + m_0^2} - m_0}{nT}\right)^{-n}, \tag{4}$$

where T is known as the inverse slope parameter, dN/dy is the ϕ-meson yield per unit rapidity, m_0 is the rest mass of ϕ meson and n is the Levy function parameter. The $\langle v_2 \rangle$

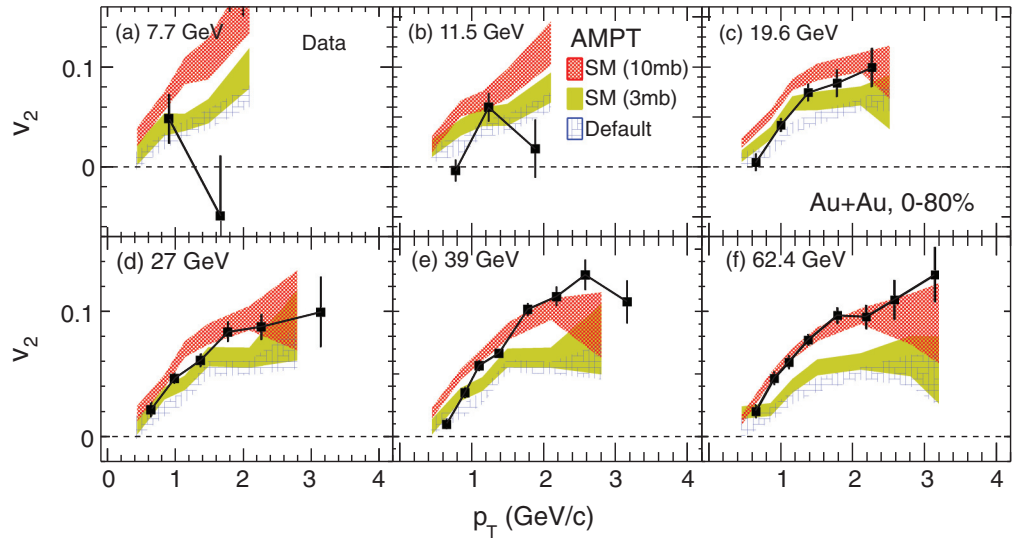

FIG. 1. (Color online) The ϕ-meson $v_2(p_T)$ for Au+Au minimum-bias collisions at mid-rapidity($|y| < 1.0$) from the STAR experiment at RHIC compared to the corresponding AMPT model calculation at various beam energies [3]. The errors shown are statistical.

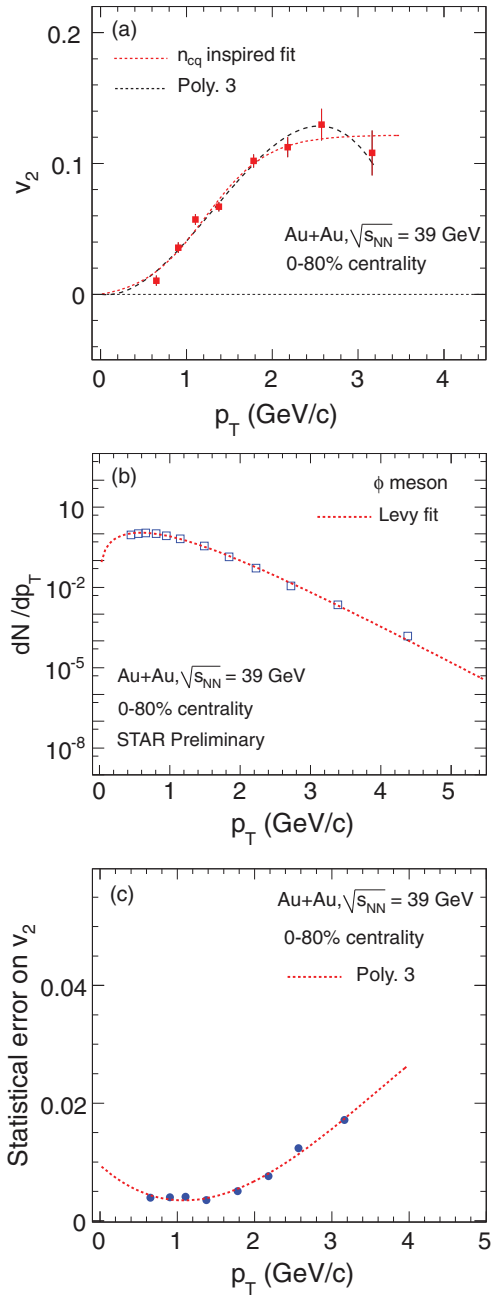

FIG. 2. (Color online) (a) The ϕ-meson $v_2(p_T)$ at $\sqrt{s_{NN}}$ = 39 GeV for 0–80 % centrality bin is fitted with a third-order polynomial (Poly. 3) and with the function described in Eq. (3). (b) The preliminary ϕ-meson dN/dp_T vs p_T at $\sqrt{s_{NN}} = 39$ GeV for 0–80 % centrality bin is fitted with a Levy function. (c) The statistical error on $v_2(p_T)$ at $\sqrt{s_{NN}} = 39$ GeV for 0–80 % centrality bin is fitted with a third-order polynomial.

for each choice of $v_2(p_T)$ parametrization is given by the integral of the corresponding distributions normalized by the integral of the p_T distribution. In addition, the $\langle v_2 \rangle$ has been calculated directly from measured data points of $v_2(p_T)$ with corresponding yield obtained from the fit function to the p_T distribution. The final $\langle v_2 \rangle$ was obtained by calculating the mean of the three $\langle v_2 \rangle$ results and the systematic error was

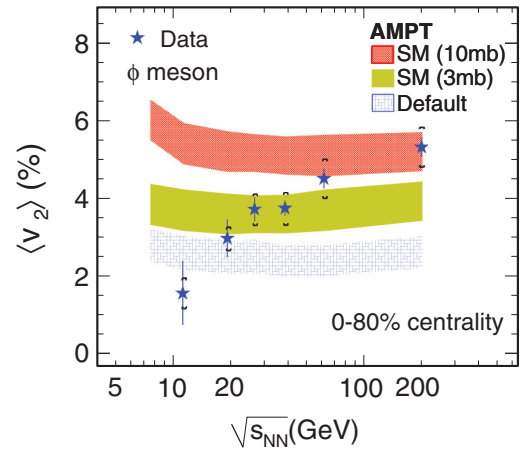

FIG. 3. (Color online) The p_T integrated ϕ-meson v_2 for Au+Au minimum-bias collisions at mid-rapidity ($|y| < 1.0$) from the STAR experiment at RHIC are compared to the corresponding AMPT model calculation at various beam energies. Systematic errors are shown by cap symbols on experimental data.

estimated from maximum deviation from the mean value. There are two sources for the statistical error: one is error on p_T distribution and other is error on $v_2(p_T)$. Since the error on dN/dp_T is very small compared to that on $v_2(p_T)$, one can simply neglect the error of dN/dp_T. Hence, only errors on $v_2(p_T)$ are taken into account for calculation of the final statistical error on $\langle v_2 \rangle$. The errors on v_2 are parameterized as a function of p_T and extrapolated to low and high p_T as shown in panel (c) of Fig. 2. Figure 2 is repeated for all the energies studied. For $\langle v_2 \rangle$ calculation in data, the final ϕ mesons spectra and $v_2(p_T)$ at 62.4 and 200 GeV published by STAR have been used [28]. For the other energies, the STAR preliminary spectra [29] and final $v_2(p_T)$ [3] have been used.

The p_T integrated ϕ-meson v_2 for Au+Au minimum-bias collisions at mid-rapidity($|y| < 1.0$) are compared to the corresponding AMPT model calculation at various beam energies in Fig. 3. In contrast to observations from the data, the $\langle v_2 \rangle$ values from the model remain constant for all the energies for a given parton-parton interaction cross section. The $\langle v_2 \rangle$ of ϕ mesons for $\sqrt{s_{NN}} \geqslant 19.6$ can be explained by the AMPT with string melting depending on parton-parton cross section. The AMPT-SM model with 10 mb parton-parton cross section explains the data very well at $\sqrt{s_{NN}} = 62.4$ and 200 GeV, whereas a 3 mb parton-parton cross section is sufficient to describe the data at $\sqrt{s_{NN}} = 19.6$, 27, and 39 GeV. On the other hand, both the AMPT-SM and AMPT default model overpredict data at $\sqrt{s_{NN}} = 11.5$ GeV, indicating negligible contribution of the partonic collectivity to the final collectivity. Due to very small statistics at $\sqrt{s_{NN}} = 7.7$ GeV, $\langle v_2 \rangle$ are not shown here. The observation that different parton-parton cross sections are needed to explain the data within the transport model framework indicates that the η/s changes with beam energy. The higher the cross section, the smaller is the η/s expected for the system. This qualitative observation of variation in the value of η/s with beam energy is consistent with the expectations from various calculations as reported in [30].

From Fig. 3, one can conclude that, as the energy decreases, contribution to the collectivity from the partonic phase also decreases, and for $\sqrt{s_{NN}} \leqslant 11.5$ GeV the hadronic interaction plays a dominant role in experimentally observed data.

IV. SUMMARY AND CONCLUSION

In summary, a compilation of the available data for elliptic flow of ϕ mesons has been presented. The implications of these results on the quark-hadron phase transition have been discussed by comparing experimental data with the AMPT model. The AMPT model with string melting scenario quantitively explains the data at $\sqrt{s_{NN}} \geqslant 19.6$ GeV by varying the parton-parton interaction cross section from 3 mb to 10 mb. The AMPT default model underpredicts that experimental data for $\sqrt{s_{NN}} \geqslant 19.6$ GeV. This tells us that there is a substantial contribution of partonic collectivity to the final collectivity for $\sqrt{s_{NN}} \geqslant 19.6$ GeV. However, both the AMPT-SM and AMPT default models cannot explain the trend of ϕ-meson v_2 as function of p_T at $\sqrt{s_{NN}} = 7.7$ and 11.5 GeV. Also the $\langle v_2 \rangle$ from AMPT default overpredicts the data at $\sqrt{s_{NN}} = 11.5$ GeV. This indicates that a possible turn-off of partonic interaction starts at $\sqrt{s_{NN}} \leqslant 11.5$ GeV. Due to the large statistical error on ϕ v_2 at $\sqrt{s_{NN}} = 7.7$ GeV, it is not possible to make any conclusions. The comparison of the experimental data on the beam energy dependence of the average elliptic flow of ϕ mesons with the corresponding results from a transport model calculation with varying parton-parton cross section suggests that the partonic contribution to the collectivity decreases and possibly the value of the η/s of the system increases as the beam energy decreases. The ϕ-meson v_2 measurement should be one of the main focuses in the proposed BES phase II program and also in the FAIR experiment at GSI to explore the phase diagram further.

ACKNOWLEDGMENTS

I thank Dr. Bedangadas Mohanty for useful discussions and help in the preparation of the manuscript. Financial support from the DST SwarnaJayanti project, Government of India, is gratefully acknowledged.

[1] I. Arsene *et al.* (BRAHMS Collaboration), Nucl. Phys. A **757**, 1 (2005); B. B. Back *et al.* (PHOBOS Collaboration), *ibid.* **757**, 28 (2005); J. Adams *et al.* (STAR Collaboration), *ibid.* **757**, 102 (2005); K. Adcox *et al.* (PHENIX Collaboration), *ibid.* **757**, 184 (2005).
[2] L. Adamczyk *et al.* (STAR Collaboration), Phys. Rev. C **86**, 054908 (2012).
[3] L. Adamczyk *et al.* (STAR Collaboration), Phys. Rev. C **88**, 014902 (2013).
[4] L. Adamczyk *et al.* (STAR Collaboration), Phys. Rev. Lett. **110**, 142301 (2013).
[5] B. I. Abelev *et al.* (STAR Collaboration), Phys. Rev. C **81**, 024911 (2010).
[6] P. F. Kolb and U. Heinz, Nucl. Phys. A **715**, 653c (2003).
[7] D. Teaney, J. Lauret, and E. V. Shuryak, Phys. Rev. Lett. **86**, 4783 (2001).
[8] P. F. Kolb and U. Heinz, in *Quark Gluon Plasma 3*, edited by R. C. Hwa and X. N. Wang (World Scientific, Singapore), pp. 634–714 [arXiv:nucl-th/0305084].
[9] P. F. Kolb *et al.*, Phys. Lett. B **500**, 232 (2001).
[10] H. Sorge, Phys. Rev. Lett. **78**, 2309 (1997).
[11] A. M. Poskanzer and S. A. Voloshin, Phys. Rev. C **58**, 1671 (1998).
[12] B. Zhang *et al.*, Phys. Lett. B **455**, 45 (1999).
[13] D. Molnar and S. A. Voloshin, Phys. Rev. Lett. **91**, 092301 (2003).
[14] J. Adams *et al.* (STAR Collaboration), Phys. Rev. Lett. **92**, 052302 (2004).
[15] C. Nonaka *et al.*, Phys. Lett. B **583**, 73 (2004); V. Greco *et al.*, Phys. Rev. C **68**, 034904 (2003); R. J. Fries *et al.*, Ann. Rev. Nucl. Part. Sci. **58**, 177 (2008).
[16] B. I. Abelev *et al.* (STAR Collaboration), Phys. Rev. Lett. **99**, 112301 (2007).
[17] P. P. Bhaduri and S. Chattopadhyay, Phys. Rev. C **81**, 034906 (2010).
[18] K. J. Wu *et al.*, Nucl. Phys. A **834**, 303c (2010).
[19] M. Bleicher and X. Zhu, Eur. Phys. J. C **49**, 303 (2007).
[20] A. Shor, Phys. Rev. Lett. **54**, 1122 (1985); J. Rafelski and B. Muller, *ibid.* **48**, 1066 (1982).
[21] Md. Nasim, B. Mohanty, and N. Xu, Phys. Rev. C **87**, 014903 (2013).
[22] B. Mohanty and N. Xu, J. Phys. G **36**, 064022 (2009).
[23] Z.-W. Lin and C. M. Ko, Phys. Rev. C **65**, 034904 (2002); Z.-W. Lin *et al.*, *ibid.* **72**, 064901 (2005); L.-Wen Chen *et al.*, Phys. Lett. B **605**, 95 (2005).
[24] X. N. Wang and M. Gyulassy, Phys. Rev. D **44**, 3501 (1991).
[25] B. Zhang, Comput. Phys. Commun. **109**, 193 (1998).
[26] B. Andersson *et al.*, Phys. Rep. **97**, 31 (1983).
[27] X. Dong *et al.*, Phys. Lett. B **597**, 328 (2004).
[28] B. I. Abelev *et al.* (STAR Collaboration), Phys. Rev. C **79**, 064903 (2009).
[29] X. Zhang (for the STAR collaboration), Nucl. Phys. A **904**, 543c (2013); Md. Nasim (STAR collaboration), PoS (**CPOD 2013**) 049 (2013).
[30] S. Plumari *et al.*, arXiv:1304.6566; R. A. Lacey *et al.*, arXiv:1305.3341; L. P. Csernai *et al.*, Phys. Rev. Lett. **97**, 152303 (2006); R. A. Lacey *et al.*, *ibid.* **98**, 092301 (2007).